applied sciences

MDPI

Article

The Effects of Methane Storage Capacity Using Upgraded Activated Carbon by KOH

Jung Eun Park, Gi Bbum Lee, Sang Youp Hwang, Ji Hyun Kim, Bum Ui Hong, Ho Kim and Seokhwi Kim *

Center for Plant Engineering, Institute for Advanced Engineering, Yongin-si 17180, Korea; jepark0123@gmail.com (J.E.P.); mnbbv21c@gmail.com (G.B.L.); syhwang80@iae.re.kr (S.Y.H.); jhkim2017@iae.re.kr (J.H.K.); buhong@iae.re.kr (B.U.H.); kimh0505@iae.re.kr (H.K.)
* Correspondence: shkim5526@iae.re.kr; Tel.: +82-31-330-7203

Received: 10 August 2018; Accepted: 28 August 2018; Published: 9 September 2018

Abstract: In this study, a feasible experiment on adsorbed natural gas (ANG) was performed using activated carbons (ACs) with high surface areas. Upgraded ACs were prepared using chemical activation with potassium hydroxide, and were then applied as adsorbents for methane (CH_4) storage. This study had three principal objectives: (i) upgrade ACs with high surface areas; (ii) evaluate the factors regulating CH_4 adsorption capacity; and (iii) assess discharge conditions for the delivery of CH_4. The results showed that upgraded ACs with surface areas of 3052 m^2/g had the highest CH_4 storage capacity (0.32 g-CH_4/g-ACs at 3.5 MPa), which was over two times higher than the surface area and storage capacity of low-grade ACs (surface area = 1152 m^2/g, 0.10 g-CH_4/g-ACs). Among the factors such as surface area, packing density, and heat of adsorption in the ANG system, the heat of adsorption played an important role in controlling CH_4 adsorption. The released heat also affected the CH_4 storage and enhanced available applications. During the discharge of gas from the ANG system, the residual amount of CH_4 increased as the temperature decreased. The amount of delivered gas was confirmed using different evacuation flow rates at 0.4 MPa, and the highest efficiency of delivery was 98% at 0.1 L/min. The results of this research strongly suggested that the heat of adsorption should be controlled by both recharging and discharging processes to prevent rapid temperature change in the adsorbent bed.

Keywords: adsorbed natural gas; activated carbon; potassium hydroxide; heat of adsorption; gas delivery

1. Introduction

The use of alternative energies, such as hydrogen (H_2) and methane (CH_4), has been studied. Studies on H_2 are usually focused on the production process [1–3], while those on CH_4 are mainly concentrated on its storage and transport. Methane is one of the most significant sources of energy from natural or purified biogas due to large resources with minimal environmental impacts. Liquefaction and compression techniques are generally applied for the storage of natural gas, but these are not practical for transportation purposes as automobile fuels because they require additional systems to lower the temperature to 111 K for liquefaction and pressurization over 20 MPa for compressing natural gas [4,5].

As an alternative method for natural gas storage, adsorbed natural gas (ANG) systems, which can store natural gas at a relatively lower pressure (3–4 MPa), have been considered and intensively studied [6–10]. The CH_4 storage capacity is the same or even higher than that of compressed natural gas (CNG) at 20 MPa. Since adsorption of CH_4 involves the interaction between the gas phase and adsorbents at a certain pressure, the gas storage capacity is strongly dependent on the adsorbent's

surface area and pore structures. Previous researchers have studied adsorbents such as activated carbon (AC), high surface activated carbon (HSAC), metal organic frameworks (MOF), and active carbon fiber [11,12]. Among the various adsorbents, activated carbons (ACs) have been considered the most suitable adsorbents due to their high surface area, microporosity, and regenerative capacity [13–15]. In this respect, previous works have been conducted to enhance the properties of adsorbents with high surface areas to develop micropores using physical and chemical activation [16]. In the literature, there are few studies on physical activation using steam or carbon dioxide (CO_2), and on chemical activation using potassium hydroxide (KOH), potassium chloride (KCl), phosphoric acid (H_3PO_4), etc. [17–19]. Particularly, the CH_4 storage capacity of activated carbon by H_3PO_4 (14 mmol CH_4/g-AC) followed by chemical activation is higher than that of KCl (9 mmol CH_4/g-AC) [8]. Lu et al. [20] mentioned that the diffusion rate of the potassium in KOH is more effective than the potassium in K_2CO_3 due to high micropore volume and a larger surface area [21–23].

One of the difficulties in ANG techniques is the management of thermal effects. The heat of adsorption significantly affects ANG storage capability even for adsorbents with high surface areas. According to the computational results of Mota et al., it was suggested that gas should be cooled before it is injected into vessels filled with adsorbents [24]. Owing to adsorbents having poor thermal conductivity, heat transfer to the surroundings is limited. Thus, it can lead to the suppression of adsorption storage capacity. According to the experimental results from Chang and Talu [25], gas delivery capacity decreased by more than 8% when the temperature decreased to 268 K, and its dynamic loss fluctuated from 15 to 25% due to changes in the heat capacity of the carbon bed. Thus, many researchers have developed transient heat and mass transfer models to simulate the performance of adsorption systems [26–28]. For instance, Ybyraiymkul et al. [27] proposed an ANG cylinder with water passing through the tubes to effectively control the heat of adsorption.

In addition, heat transfer on the adsorbent has an influence on gas delivery during discharge. The heat of adsorption generally decreases during the discharge. Thus, the amount of delivered gas decreases when the discharge flowrate is higher. Due to these reasons, a large amount of natural gas still remained after discharging in the previous adsorption systems. Currently, to overcome the limitations, MOF with flexible structures have been developed [29]. The pores in the MOF structure were expanded at a certain pressure, and then the gases were adsorbed in the pores. On the other hand, the adsorbents were desorbed from inside the pores while shrinking the pore structure at low pressure. MOF have advantages for both adsorption and desorption of methane, but it is not yet commercially developed and is also expensive [30]. NGVs (natural gas vehicles) with an adsorption system require a large amount of adsorbents, leading to a high price. Using ACs for the adsorption system is much cheaper than MOF, and is already commercialized. If the heat generation and discharging conditions in the ANG system are controlled and optimized, respectively, this system with ACs can be used in NGVs and for various other applications as well.

This study was performed (i) to evaluate the CH_4 adsorption capacity in various conditions and (ii) to optimize the discharge conditions for the delivery of CH_4. In more detail, upgraded ACs with a high surface area were produced by chemical activation and were applied in an ANG system. In addition, ANG experiments were performed with different conditions, such as temperature and pressure, and were compared with the amount of available CH_4 at different discharge rates.

2. Materials and Methods

2.1. Preparation of Activated Carbons

Two types of commercial ACs (wood: JIG-SC-2040, Ja Yeon Science Ind. Co., Chulwon, Korea; coconut: LGL-100, Daelim Carbon Ind. Co., Seoul, Korea) were utilized as precursors for this study. To upgrade the low-grade AC, 1 kg of AC was treated with potassium hydroxide (KOH, Samchun chemical, Seoul, Korea) and the mass ratio of AC:KOH was 1:2 under an inert environment. After the chemical activation, the average particle size of the upgraded ACs was around 500 μm.

The mixture was put into a tubular furnace under N_2 flow and heated to 1123 K at a rate of 10 K/min, and then held for 3 h, as described in a previous study [31]. After completion of the activation processes, the prepared AC was washed with deionized water until the pH was neutral, and was subsequently dried at 378 K. The commercial ACs based from wood and coconut were denoted as AC-WR and AC-CR, respectively. The chemically activated ACs using the commercial ACs were also denoted as AC-WA and AC-CA, respectively (AC: activated carbon, W: wood based, C: coconut based, R: raw/commercial materials, and A: activation).

2.2. Analytical Methods for Determining the Chemical Properties of Activated Carbons

For the proximate analysis, the dried samples were put into a furnace (Daeheung Science, DF-4S, Korea) and heated at 1223 K for 7 min. The weight loss of the samples was measured for volatile matter. The samples were put into the furnace again and heated at 1023 K for 10 h to measure the amount of weight loss for fixed carbon and the residual for ash contents. The ash, volatile matter, and fixed C contents within the ACs were considered as a percentage of the weight. The elemental (C, H, O, N, and S) contents were determined using an elemental analyzer (FLASH 2000, Thermo Fisher Scientific, Waltham, MA, USA), and the results are listed in Table 1. The surface area of the AC was measured using the Brunauer-Emmett-Teller (S_{BET}) method based on the N_2 adsorption at 77 K, which was measured using an adsorption analyzer (ASAP-2010, Micromeritics Inc., Norcross, GA, USA). The pore volume (V) of the AC was calculated according to the t-plot method for micropores (<2 nm) and the Barrett Joyner and Halenda method for mesopores (>2 nm), respectively. Before carrying out the N_2 isotherms, samples were outgassed at 623 K to a constant vacuum (P/P_0: 2 μmHg) for 360 min. To investigate the surface morphologies of ACs with and without chemical activation by KOH, a field-emission scanning electron microscope (FE-SEM; S-4300, Hitachi Co, Tokyo, Japan) was used.

Table 1. Ultimate and proximate analysis of ACs (activated carbons) as precursors. AC-WR: the commercial ACs based on wood material, AC-CR: the commercial ACs based on coconut material, n.d.: not detected.

Sample	Ultimate Analysis (wt.%)					Proximate Analysis (wt.%)		
	Carbon	Hydrogen	Oxygen	Nitrogen	Sulfur	Volatile	Fixed Carbon	Ash
AC-WR	71.60	1.60	17.20	0.80	n.d.	18.56	74.68	6.76
AC-CR	89.03	0.30	2.50	0.00	n.d.	5.14	92.73	2.12

2.3. Adsorbed Natural Gas System Experiments

The ANG system consisted of a compressor with an adjustable flow rate and a prototype storage cylinder with a volume of 50 mL (Diameter: 40 mm; Height: 40 mm) that was filled to maximum capacity. Using this system, the CH_4 storage capacity was evaluated as a function of pressure up to 20 MPa. In the charge period, the CH_4 gas was maintained at a constant pressure with a pressure regulator. The weight of the reactor filled with ACs was measured using a balance, and the CH_4 was sufficiently adsorbed in the reactor. The weight difference was the amount of CH_4 adsorbed. The desorption of CH_4 was then tested in atmosphere (101 kPa) and vacuum conditions (20 kPa) with a discharge flow rate of 0.5 L/min. After the desorption process, the weight of the reactor with ACs was measured again using the balance. The weight differences indicated the amount of CH_4 desorbed. In the ANG system, deliverability, which represents useable gas capacity, is one of the main factors in the application. It can be defined as the difference in the amount of CH_4 between adsorption at the target storage pressure and the residual after desorption. To evaluate delivery capacity, discharge flow rates were regulated with a flowrate of 0.1 and 0.5 L/min at 0.4 MPa, respectively. A CNG experiment in the absence of absorbents was also performed as a function of pressure up to 20 MPa for comparison.

3. Results

3.1. Upgrading Activated Carbons

Elemental contents, such as C, H, O, N, and S, were different in the precursors of wood and coconut (Table 1).

C contents were relatively high in the samples from coconuts, while H and O were relatively more concentrated in the wood samples. Similarly, the level of volatile matter in the wood samples was 2.5 times higher than in the coconut samples. The molar ratio of O/C, which is indicative of oxygenated functional groups (OFGs), of the wood samples was eight times higher than that of coconut samples. OFGs, as electron donors, may accelerate the redox reaction more easily than elemental C when chemical activation with KOH is applied. Thus, pore development on the surface of the wood samples would be more enhanced [32,33].

N_2 adsorption and desorption isotherms of ACs followed the type I isotherms regardless of activation with KOH, as shown in Figure 1a,b.

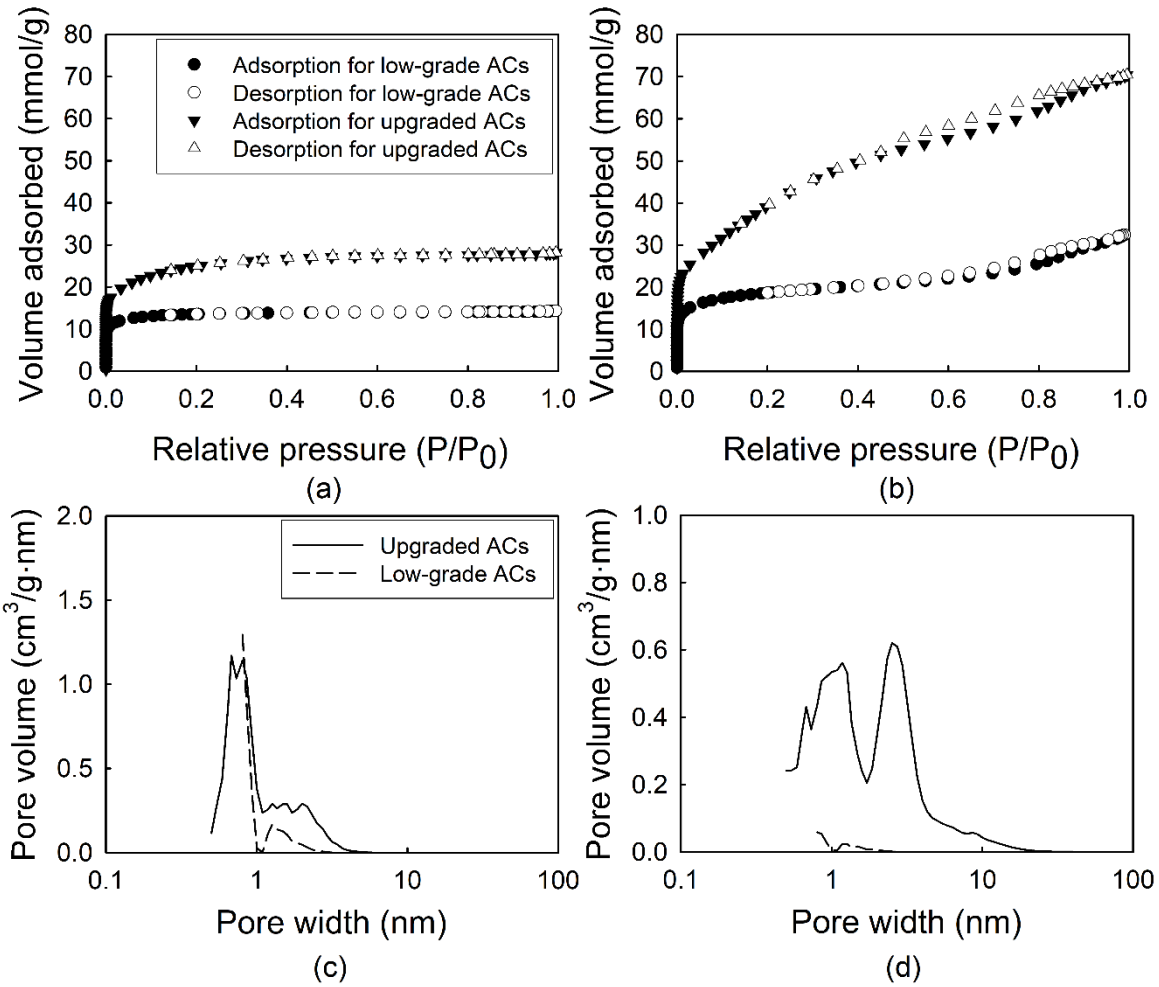

Figure 1. Nitrogen ad-/de-sorption isotherms and pore size distribution for coconut (**a**,**c**) and wood (**b**,**d**) based ACs (activated carbons). These ACs were classified into low and upgraded without/with KOH treatment.

As shown in Figure 1a,b and Table 2, the surface area and micropore volume of wood based ACs (AC-WR and AC-WA) were higher than coconut based ACs (AC-CR and AC-CA). After activation, the surface area of upgraded ACs was over two times higher than that of raw-graded ACs. In the adsorption and desorption isotherms of the adsorbents, the hysteresis loop in the relative pressure

(P/P_0) range of 0.4–1.0 was indicative of the mesoporosity of ACs. In the case of AC-WA, the fraction of mesoporosity was rapidly increased compared to AC-WR. However, in the case of AC-C, the 24.5% fraction of mesoporosity was increased to 47.5% after upgrading. The pore size distribution of the adsorbents clearly showed that the mesopores had a broad pore size distribution (Figure 1c,d). All samples dominantly developed micropores, but the mesopore fractions increased after KOH treatment. The surface areas (S_{BET}) of the upgraded samples (AC-WA and AC-CA) increased significantly, and were over two times greater than those of the precursors (Table 2 and Figure 1).

Table 2. Textural properties and methane storage capacity.

Sample	S_{BET} (m^2g^{-1})	V_{Micro} (cm^3g^{-1})	V_{Meso} (cm^3g^{-1})	R_{micro} (%)	R_{meso} (%)	Methane Storage Capacity (g-CH_4/g-AC)
AC-WR	1152	0.50	0.59	46.1	53.9	0.17
AC-WA	3052	0.04	2.37	1.73	98.3	0.32
AC-CR	1068	0.35	0.11	75.5	24.5	0.11
AC-CA	2258	0.48	0.43	52.5	47.5	0.25

We observed the adsorbents with an FE-SEM to investigate their morphologies, as shown in Figure 2. SEM images of the activated adsorbents (AC-WA and AC-CA) revealed rough surfaces caused by pore generation.

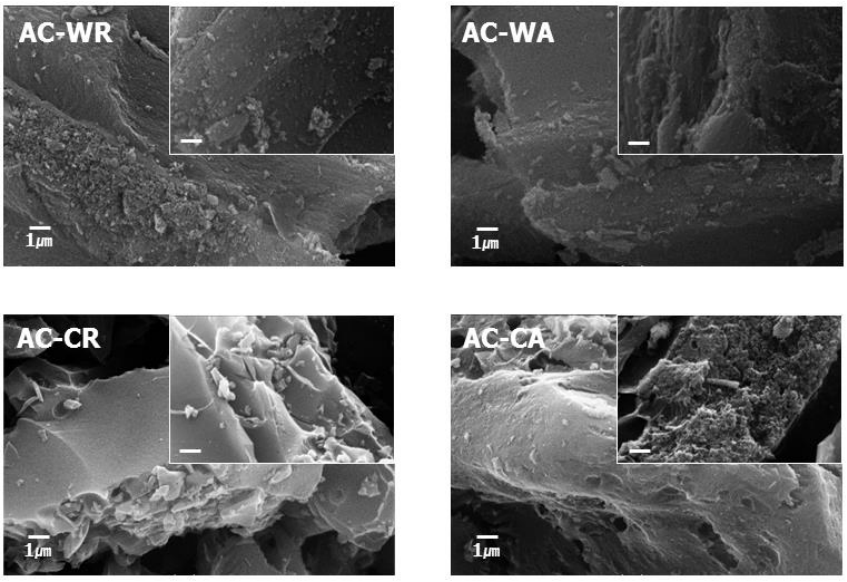

Figure 2. SEM image of altered carbon (AC) such as AC-WR, AC-WA, AC-CR, and AC-CA.

3.2. Characteristics of CH_4 Storage by Compressed and Adsorbed

Figure 3a shows the CH_4 storage capacity as a function of pressure under a compressed system. The storage capacity of CH_4 increased with pressure; the storage capacity was 0.176 g-CH_4/mL at 20 MPa, which was beyond the expectation (0.131 g-CH_4/mL) because of the compression properties (Z-factor of 0.84 at 298 K) of CH_4 [34].

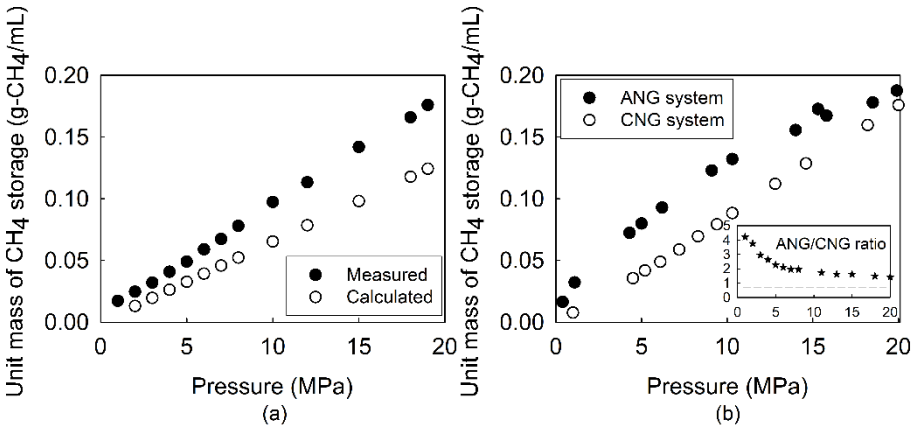

Figure 3. (**a**) Comparison of measured methane storage in the reactor and the calculated methane amount based on the reactor volume at different pressures using the ideal gas law; and (**b**) comparison of methane storage between adsorbed natural gas (ANG) and compressed natural gas (CNG) at different pressures (inset Figure 3b illustrating the ratio for ANG/CNG).

On the other hand, the CH_4 storage capacities of the ANG system under the given pressure conditions were up to 20 MPa higher than those of the CNG system (Figure 3b). The CH_4 storage capacity at a pressure of less than 6 MPa was over two times higher than that of the CNG system (Figure 3b), while it became close to the capacity of the CNG system towards a pressure of 20 MPa. The parabolic CH_4 storage trend in the ANG system at a relatively lower pressure strongly indicated that the number of active sites that adsorb CH_4 molecules is one of the most important adsorbent properties.

3.3. Methane Storage Capacity at Different Conditions

Adsorbents are mainly affected by the surface area, pore size distribution, and packing density. These factors should be addressed to achieve higher storage capacity in the ANG system [4,11,35]. Among these factors, the surface area seems to primarily affect the CH_4 storage capacity. Figure 4a clearly shows a positive correlation between the surface area and the CH_4 storage capacity, as shown in previous studies [7,36,37].

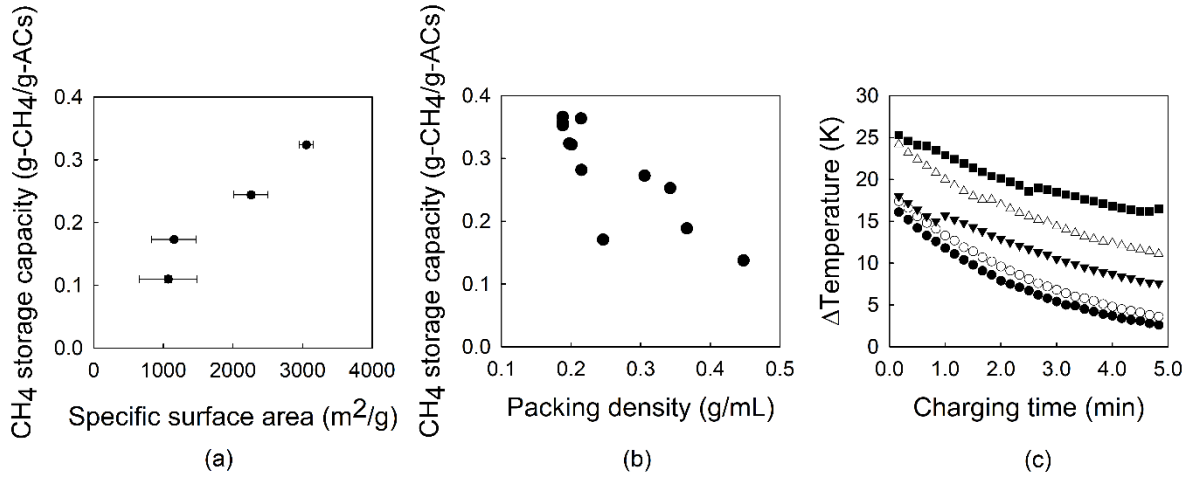

Figure 4. Influence of (**a**) the methane storage capacity on the surface area over upgraded ACs. Di-directional error bars show standard deviation for the CH_4 storage capacity and the surface area of ACs; (**b**) the unit mass of the adsorbed on the packing density of the AC-WA (3052 m^2/g); and (**c**) the differential temperature as a function of adsorption time with each adsorbed pressure (●: 2.0 MPa, ○: 5.0 MPa, ▼: 6.0 MPa, △: 7.0 MPa, ■: 20 MPa), with a flow rate of 0.5 L/min over AC-WA (3052 m^2/g).

By using upgraded ACs (AC-WA) in ANG experiments at 3.5 MPa in this study, the CH_4 storage capacity of upgraded samples increased by 59.6% for AC-WR (0.273 g-CH_4/g-ACs) compared with the low-grade sample (0.171 g-CH_4/g-ACs). However, its capacity did not show a positive relationship with the packing density (Figure 4b). As mentioned previously, the increase in the number of adsorption sites could lead to the enhanced CH_4 storage capacity in the ANG tank. However, this adsorption process entails an exothermic reaction, so the decreasing patterns of CH_4 storage capacity in Figure 4b could be explained by the increase in packing density. The heat control of adsorption plays an important role in gas storage because it significantly affects adsorption rates. Experimental and modeled results from Yue et al. revealed that the temperature induced by the heat of adsorption at the beginning of the adsorption experiment increased sharply and reached up to 14 K of temperature difference using a coal sample [28]. A few studies on the heat of adsorption according to various pressures, and even on CH_4 stored under compression, were reported in the literature. The temperature difference (ΔT) inside the reactor decreased as the pressure decreased, as shown in Figure 4c. At the beginning of adsorption, the rapid increase in ΔT influenced the CH_4 adsorption capacity.

Heat transfer accompanied adsorption. Thus, the temperature of the adsorbent bed had a significant influence on the ANG storage system. We investigated the CH_4 storage as a function of adsorption temperature, as shown in Figure 5. The results showed that the CH_4 capacity in AC-WA increased at low adsorption temperatures. The residual amount of CH_4 after atmospheric pressure (101 kPa) desorption showed that the residual CH_4 increased from 15 to 20% as the temperature decreased. In the vacuum desorption, residual CH_4 increased from 5 to 10% as the temperature decreased. The residues were dependent on both the desorption temperature and pressure.

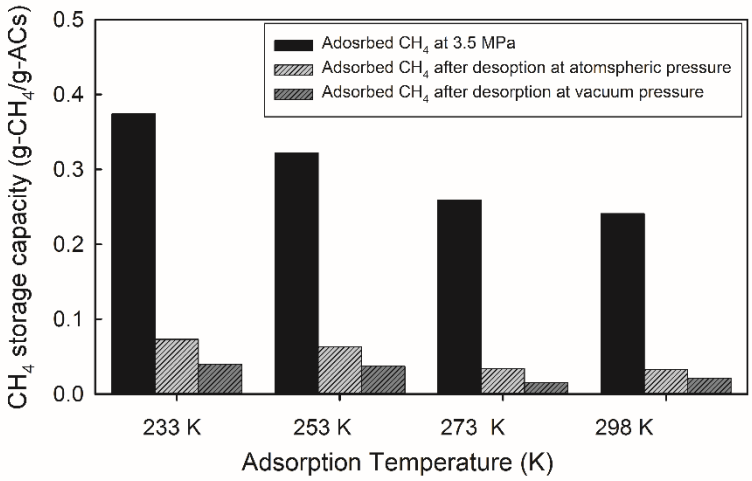

Figure 5. Methane storage and residual capacity as a function of adsorption/desorption temperature for AC-WA. All adsorption experiments were performed at 3.5 MPa and with 12.0 g of AC.

3.4. Gas Delivery

Previous research has only addressed the enhancement of storage efficiency without considering gas delivery, which is the amount of gas available under certain circumstances using porous adsorbents. The CH_4 storage capacity is not equal to useable gas capacity due to the strong interaction with the adsorbents [36]. To provide intensive research, we confirmed that gas delivery after adsorption depended on the discharge rates (0.1 L/min, 0.5 L/min) at 0.4 MPa after adsorption at 10 MPa (Figure 6).

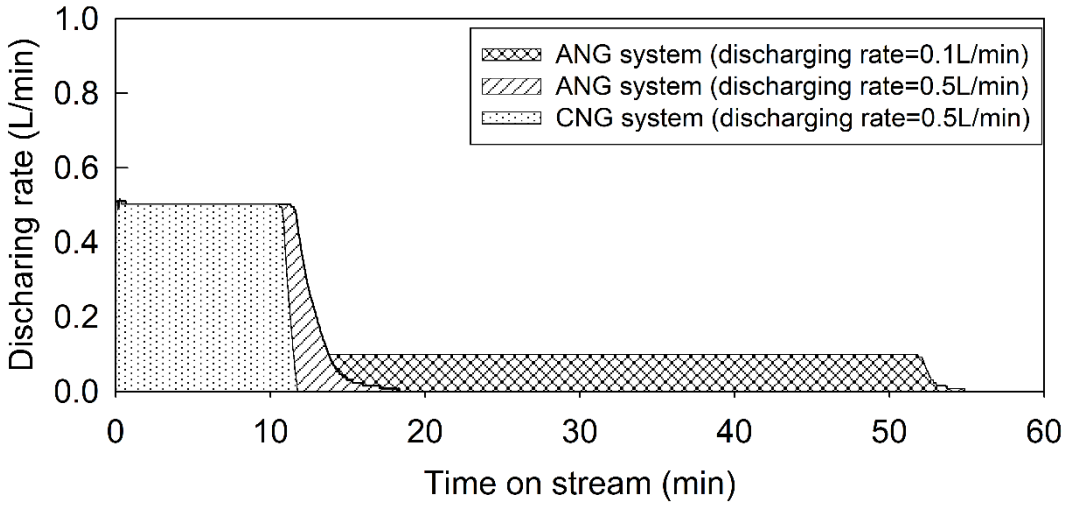

Figure 6. Variation of delivery capacity with specific flow rate for constant pressure charging.

A CNG experiment was conducted at 0.5 L/min for comparison. The accessible CH_4 varied with different discharge rates. Useable masses of CH_4 after delivery of ANG were much higher than those in the CNG system. For instance, the mass of available CH_4 in the ANG system was 6.8% higher than in the CNG system at a constant flow rate (0.5 L/min, 0.4 MPa). In addition, the storage capacity in the presence of ACs was 25.4% higher than in the CNG system at the same pressure of 10 MPa (Figure 3b) and also the useable CH_4 in ANG was higher, as mentioned previously. Both the high storage capacity and the discharging rate of CH_4 in the ANG system lead to the high gas delivery.

In the ANG system, deliverable CH_4 became greater when the discharge rates decreased. Over 87% (6.22 L) of total adsorbed CH_4 could be delivered at a discharge rate of 0.5 L/min, while over 98% of CH_4 (7.01 L) was available at 0.1 L/min. This was because of the changes in the heat of the carbon bed during CH_4 discharge. During the gas discharge, the temperature of the carbon bed might have cooled, thereby reducing the CH_4 delivery capacity. Zakaria and George also reported that the delivery capacity was highly influenced by the carbon bed temperature [38]. Thus, a heating system could be introduced to improve the CH_4 delivery capacity during discharge periods.

4. Conclusions

This work aimed to determine the most efficient storage of CH_4 gas using an ANG system. An upgraded adsorbent was applied in the ANG system, and the efficiency was tested under various conditions, such as temperature, pressure, and discharge flow rate. To upgrade the adsorbents, ACs were chemically activated with KOH, thereby resulting in a high surface area (3052 m^2/g) with a micropore volume of 0.58 cm^3/g. The surface area of the ACs increased with increasing CH_4 storage. Among them, AC-WA with a high surface area showed the highest storage value of 0.32 g-CH_4/g-AC.

The heat of adsorption significantly influenced the amount of adsorbed and/or desorbed CH_4 in the ANG system. During the adsorption of CH_4 gas, the exothermic temperature should be suppressed to increase the adsorption amount. The amount of discharged CH_4 increased as the temperature increased. The results also confirmed that CH_4 capacity was controlled by heat during both recharging and discharging conditions. These results could form the foundation for the practical application of the ANG system.

Author Contributions: S.K., J.E.P. and H.K. conceived and designed the experiments; J.E.P. and S.K. drafted the manuscript; J.E.P., G.B.L. and S.Y.H. performed the experiments; J.H.K., G.B.L. upgraded the activated carbons; J.H.K. analyzed the data; B.U.H. and H.K funded this works; S.Y.H., S.K. and J.E.P. wrote and revised the paper.

Funding: This study was supported by the Energy Development Technology Program of the Korea Institute of Energy Technology Evaluation and Planning (KETEP) granted financial resource from the Ministry of Trade, Industry & Energy, Republic of Korea (Project No. 20162010104680) and also the National Research Foundation of

Korea(NRF) and the Center for Women In Science, Engineering and Technology(WISET) Grant funded by the Ministry of Science and ICT under the Program for Returners into R&D.

Acknowledgments: The authors thank the reviewers for their valuable comments and suggestions, which improved the technical content and the presentation of the paper.

Conflicts of Interest: The authors declare no conflicts of interest.

References

1. Bartocci, P.; Zampilli, M.; Bidini, G.; Fantozzi, F. Hydrogen rich gas production through steam gasification of charcoal pellet. *Appl. Therm. Eng.* **2018**, *132*, 817–823. [CrossRef]
2. Hawkes, F.R.; Dinsdale, R.; Hawkes, D.L.; Hussy, I. Sustainable fermentative hydrogen production: Challenges for process optimisation. *Int. J. Hydrog. Energy* **2002**, *27*, 11–12. [CrossRef]
3. Nikolaidis, P.; Poullikkas, A. A complarative overview of hydrogen production processes. *Renew. Sustain. Energy Rev.* **2016**, *67*, 597–611. [CrossRef]
4. Lozano-Castello´a, D.; Alcaniz-Monge, J.; de la Casa-Lillo, M.A.; Cazorla-Amoro´s, D.; Linares-Solano, A. Advances in the study of methane storage in porous carboneous materials. *Fuel* **2002**, *81*, 1777–1803. [CrossRef]
5. Ou, X.M.; Zhang, X.L.; Zhang, X.; Zhang, Q. Life cycle GHG of NG-based fuel and electric vehicle in China. *Energies* **2013**, *6*, 2644–2662. [CrossRef]
6. Sapag, K.; Vallone, A.; Blanco, A.G.; Solar, C. Adsorption of methane in porous materials as the basis for the storage of natural gas. In *Natural Gas*; Intech Open: London, UK, 2010; Chapter 10; pp. 205–244, ISBN 978-953-307-112-1.
7. Policicchio, A.; Filosa, R.; Abate, S.; Desiderio, G.; Colavita, E. Activated carbon and metal organic framework as adsorbent for low-pressure methane storage application: an overview. *J. Porous Mater.* **2016**, *24*, 905–922. [CrossRef]
8. Moreno-Pirajan, J.C.; Bastidas-Barrance, M.J.; Giraldo, L. Preparation of activated carbons for storage of methane and its study by adsorption calorimetry. *J. Therm. Anal. Calorim.* **2017**, *131*, 259–271. [CrossRef]
9. Choi, P.-S.; Jeong, J.-M.; Choi, Y.-K.; Kim, M.-S.; Shin, G.-J.; Park, S.-J. A review: Methane capture by nanoporous carbon materials for automobiles. *Carbon Lett.* **2016**, *17*, 18–28. [CrossRef]
10. He, Y.B.; Zhou, W.; Qian, G.D.; Chen, B.L. Methane storage in metal-organic frameworks. *Chem. Soc. Rev.* **2014**, *43*, 5657–5678. [CrossRef] [PubMed]
11. Alhasan, S.; Carriveau, R.; Ting, D.S.K. A review of adsorbed natural gas storage technologies. *Int. J. Environ. Stud.* **2016**, *73*, 343–356. [CrossRef]
12. Vasiliev, L.L.; Kanonchik, L.E.; Mishkinis, D.A.; Rabetsky, M.I. Adsorbed natural gas storage and transportation vessels. *Int. J. Therm. Sci.* **2000**, *39*, 1047–1055. [CrossRef]
13. Benaddi, H.; Bandosz, T.J.; Jagiello, J.; Schwarz, J.A.; Rouzaud, J.N.; Legras, D.; Beguin, F. Surface functionality and porosity of activated carbons obtained from chemical activation of wood. *Carbon* **2000**, *38*, 669–674. [CrossRef]
14. Ros, A.; Lillo-Rodenas, M.A.; Fuente, E.; Montes-Moran, M.A.; Martin, M.J.; Linares-Solano, A. High surface area materials prepared from sewage sludge-based precursors. *Chemosphere* **2006**, *65*, 132–140. [CrossRef] [PubMed]
15. Srinivas, G.; Burres, J.; Yildirim, T. Graphene oxide derived carbons (GODCs): Synthesis and gas adsorption properties. *Energy Environ. Sci.* **2012**, *5*, 6453–6459. [CrossRef]
16. Makal, T.A.; Li, J.-R.; Lu, W.; Zhou, H.-C. Methane storage in advanced porous materials. *Chem. Soc. Rev.* **2012**, *41*, 7761–7779. [CrossRef] [PubMed]
17. Yang, K.; Zhu, L.; Yang, J.; Lin, D. Adsorption and correlations of selected aromatic compounds on a KOH-activated carbon with large surface area. *Sci. Total Environ.* **2018**, *618*, 1677–1684. [CrossRef] [PubMed]
18. Chen, Y.; Liu, C.; Li, F.; Cheng, H.-M. Pore structures of multi-walled carbon nanotubes activated by air, CO_2 and KOH. *J. Porous Mater.* **2006**, *13*, 141–146. [CrossRef]
19. Virla, L.D.; Montes, V.; Wu, J.; Ketep, S.F.; Hill, J.M. Synthesis of porous carbon from petroleum coke using steam, potassium and sodium: Combining treatments to create mesoporosity. *Microporous Mesoporous Mater.* **2016**, *234*, 239–246. [CrossRef]

20. Lu, C.L.; Xu, S.P.; Liu, C.H. The role of K_2CO_3 during the chemical activation of petroleum coke with KOH. *J. Anal. Appl. Pyrolysis* **2010**, *87*, 282–287. [CrossRef]
21. Patil, K.H.; Sahoo, S. Charge characteristic of adsorbed natural gas storage system based on MAXSORIII. *J. Nat. Gas Sci. Eng.* **2017**, *52*, 267–282. [CrossRef]
22. Romanos, J.; Beckner, M.; Rash, T.; Firlej, L.; Kuchta, B.; Yu, P.; Suppes, G.; Wexler, C.; Pfeifer, P. Nanospace engineering of KOH activated carbon. *Nanotechnology* **2012**, *23*, 015401. [CrossRef] [PubMed]
23. Hui, T.S.; Zaini, M.A.A. Potassium hydroxide activation of activated carbon: A commentary. *Carbon Lett.* **2015**, *16*, 275–280. [CrossRef]
24. Mota, J.P.B.; Rodrigues, A.E.; Saatdjian, E.; Tondeur, D. Dynamics of natural gas adsorption storage systems employing activated carbon. *Carbon* **1997**, *35*, 1259–1270. [CrossRef]
25. Chang, K.J.; Talu, O. Behaviour and performance of adsorptive natural gas storage cylinders during discharge. *Appl. Therm. Eng.* **1996**, *16*, 359–374. [CrossRef]
26. El-Sharkawy, I.I.; Mansour, M.H.; Awad, M.M.; El-Ashry, R. Investigation of Natural Gas Storage through Activated Carbon. *J. Chem. Eng. Data* **2016**, *11*, 258–274. [CrossRef]
27. Ybyraiymkul, D.; Ng, K.C.; Kaltayev, A. Experimental and numerical study of effect of thermal management on storage capacity of the adsorbed natural gas vessel. *Appl. Therm. Eng.* **2017**, *125*, 523–531. [CrossRef]
28. Yue, G.W.; Wang, Z.F.; Tang, X.; Li, H.J.; Xie, C. Physical Simulation of Temperature Influence on Methane Sorption and Kinetics in Coal (II): Temperature Evolvement during Methane Adsorption in Coal Measurement and Modeling. *Energy Fuels* **2015**, *29*, 6355–6362. [CrossRef]
29. Li, H.; Wang, K.H.; Sun, Y.J.; Lollar, C.T.; Li, J.; Zhou, H.-C. Recent advances in gas storage and separation using metal-organic frameworks. *Mater. Today* **2018**, *21*, 108–121. [CrossRef]
30. DeSantis, D.; Mason, J.A.; James, B.D.; Houchins, C.; Long, J.R.; Veenstra, M. Techno-economic analysis of metal-organic frameworks for hydrogen and natural gas storage. *Energy Fuels* **2017**, *31*, 2024–2032. [CrossRef]
31. Lee, G.B.; Jung, H.S.; Hong, B.U.; Kim, S.H.; Choi, S.S. Optimization of washing process for the recycling of potassium in the manufacturing of activated carbon. *J. Korean Org. Resour. Recyc. Assoc.* **2017**, *25*, 63–71, (Korean with English abstract).
32. Jian, A.; Balasubramanian, R.; Srinivasan, M.P. Hydrothermal conversion of biomass waste to activated carbon with high porosity: A review. *Chem. Eng. J.* **2016**, *283*, 789–805. [CrossRef]
33. Molina-Sabio, M.; Rodriguez-Reinoso, F. Role of chemical activation in the development of carbon porosity. *Colloid Surf. A* **2004**, *241*, 15–25. [CrossRef]
34. Yang, S.L. Natual gas physical properties under high pressure. In *Fundamental of Petrophysics*, 2nd ed.; Springer: Berlin, Germany, 2017; pp. 34–35, ISBN 978-3-662-55028-1.
35. Travis, W.; Gadipelli, S.; Guo, Z.X. Superior CO_2 adsorption from waste coffee ground derived carbons. *RSC Adv.* **2015**, *5*, 29558–29562. [CrossRef]
36. Judd, R.W.; Gladding, D.T.M.; Hodrien, R.C.; Bates, D.R.; Ingram, J.P.; Allen, M. The Use of a Natural Gas Technology for Large Scale Storage. 1992; pp. 575–579. Available online: http://web.anl.gov/PCS/acsfuel/preprint%20archive/Files/43_3_BOSTON_08-98_0575.pdf (accessed on 1 July 2018).
37. Kumar, K.V.; Preuss, K.; Titirici, M.-M.; Rodríguez-Reinoso, F. Nanoporous Materials for the Onboard Storage of Natural Gas. *Chem. Rev.* **2017**, *117*, 1796–1825. [CrossRef] [PubMed]
38. Zakaria, Z.; George, T. The performance of commercial activated carbon absorbent for adsorbed natural gas storage. *Int. J. Recent Res. Appl. Stud.* **2011**, *9*, 225–230.